FACTA UNIVERSITATIS
Series: **Electronics and Energetics** Vol. 32, N° 4, December 2019, pp. 571-579
https://doi.org/10.2298/FUEE1904571R

COMPACT LEFT-HANDED DUAL-BAND FILTERS BASED ON SHUNDTED STUB RESONATORS

Vasa Radonić, Vesna Crnojević-Bengin

University of Novi Sad, BioSense Institute – Research and Development Institute for Information Technologies in Biosystems, Novi Sad, Serbia

Abstract. *In this paper, super-compact microstrip dual-band resonator is presented, designed using the superposition of two simple left-handed (LH) resonators with single shunt stub. The proposed resonator exhibits spurious response in wide frequency range and therefore allows construction of dual-band filters using the superposition principle. The equivalent circuit model of the proposed resonator is crated and the influence of different geometrical parameters to the performances of the resonator are analyzed in details. As an examples, two dual-band filters that operate simultaneously at the WiMAX frequency bands are designed.*

Key words: *left-handed, metamaterials, microstrip resonator, dual-band resonator, dual-band filter*

1. INTRODUCTION

Increasing demands for higher capacity of various communication systems, together with the unavailability of certain portions of the frequency spectrum, have created a great need for multi-band passive filters that can simultaneously operate at several non-harmonically related frequencies. The design of compact filters that operate at two independent frequencies and exhibit independently controlled bandwidths still remains a challenge. Different dual-band filter topologies have been recently proposed based on different synthesis techniques such as dual-band frequency transformation [1], filters based on dual-mode resonators [2], stepped impedance resonators [3], etc.

Double-negative or left-handed (LH) media, that simultaneously exhibits negative values of permittivity and permeability in a certain frequency range, were attract significant attention in the last decade [4-5]. Artificial left-handed transmission lines (LH TL) allow the design of miniature passive microwave devices such as filters, antennas or directional couplers [4-8]. In [8], LH TL are implemented in microstrip architecture using unit cells comprised of one interdigital capacitor and one grounded inductive stub.

Received February 25, 2019; received in revised form April 16, 2019
Corresponding author: Vasa Radonić
University of Novi Sad, BioSense Institute – Research and Development Institute for Information Technologies in Biosystems, Zorana Đinđića 1, 21101 Novi Sad, Serbia
(E-mail: vasarad@uns.ac.rs)

Although these elements provide the LH contribution to the structure, the whole structure is in fact a composite right/left handed (CRLH) transmission line, due to the inherent parasitic series inductance and parallel capacitance of the microstrip line. Balanced CRLH lines show the unique property of achieving zero propagation constant at a nonzero frequency. By utilizing this feature, resonator called Zeroth Order Resonator (ZOR) was designed in [9]. ZOR is implemented as a microstrip line with two interdigital capacitors and one stub inductor connected to the ground plane. Its resonance is independent of the length of the structure but depends only on the reactive loading. ZOR performances are comparable to those of the conventional half-wavelength microstrip resonator on the same substrate. However, tuned to the same resonant frequency, the overall length of the ZOR is smaller and equal to $\lambda_g/5$, where λ_g is the guided wavelength.

In this paper, we propose a much simpler version of the CRLH resonator, called Single Shunt Stub Resonator (SSSR), where interdigital capacitor is replaced by a simple gap one. When tuned to the same resonant frequency as ZOR, same fractional bandwidth and insertion loss, SSSR exhibits more than three times smaller dimensions, as well as significantly better out-of-band performances. Using proposed SSSR resonators, a compact dual-band resonators are formed using superposition method. The influence of different geometrical parameters to the performances and the tuning range of the proposed dual-band resonator is analyzed in detail. Performed analysis shown that the characteristic of the each passband can be independently controlled. Such dual-band resonators are of the greatest importance for modern wireless systems, where multi-band operation on non-harmonically related frequencies is greatly needed. To demonstrate applicability of the proposed resonator, two second order dual-band filters that operates according to the IEEE WiMAX 802.16 standard are designed and compared with different dual-band filters recently proposed in literature in term of operating frequency, insertion losses and overall size.

2. SINGLE SHUNT STUB RESONATOR

End-coupled microstrip resonators employ gaps that are, in fact, serial capacitance and can be used to obtain LH behaviour. Consequently, LH resonator can be designed without interdigital capacitors used in ZOR which significantly reduces its fabrication complexity. In Fig. 1a, the proposed single shunt stub resonator (SSSR) is shown together with relevant dimensions, where g denotes gap between the microstrip line and the resonator, L is the overall length of the resonator, w is width of 50 Ω line, and L_s and w_s are length and width of the inductive stub, respectively. To allow fair comparison, the gap g and the dimension of the inductive stub L_s and w_s were optimized to achieve the same resonant frequency, same fractional bandwidth and same insertion loss at resonance as ZOR with dimensions reported in [9]. The same substrate was used for both circuits with thickness equal to 1.575 mm, dielectric constant ε_r=2.17 and dissipation factor 0.0009. Fig. 2 shows the photograph of the fabricated resonator and comparison of the SSSR and ZOR responses. The overall length of the ZOR is equal to 24.4 mm, while the proposed SSSR is only 7.5 mm long, i.e. more than three times shorter than ZOR. The simulated responses of both structures are compared in Fig. 2, where it can be seen that the SSSR exhibits second harmonic at 7.69 GHz, thus creating a wider stopband with insertion loss higher than 35 dB. This stopband presents a novel feature of SSSR, not

existing in ZOR, which exhibits second harmonic at approximately two times the resonant frequency, i.e. at 3.81 GHz. A measured response of the SSSR is as well shown in Fig. 2, illustrating a good agreement with the simulated one. Furthermore, ZOR is designed with interdigital spacing equal to 100 μm, so it cannot be coupled stronger to the feed lines (i.e. the insertion loss at resonance and the fractional bandwidth are the best achievable in standard PCB technology). For this comparison, SSSR was designed using gaps equal to 900 μm. Therefore, by decreasing the gaps, significantly stronger coupling to the feed lines and smaller insertion loss can be easily obtained.

The proposed resonator can be modelled using a standard equivalent circuit of a CLRH TL, shown in Fig. 1b, which is basically equivalent to the circuit proposed in [10] used for modelling of dual-band CRLH resonators. The inductive stub is modelled by the parallel resonant circuit with inductance L_s and capacitance C_s, while the inductance of the via is included in L_s. To better understand the behaviour of the SSSR, the values of the elements of equivalent circuit have been extracted for the lossless case using standard formulas for microstrip elements calculation. Values obtained for SSSR and ZOR are compared in the Table I. As expected, it can be seen that the SSSR exhibits much lower series capacitance than ZOR, but significantly increased shunt inductance. In both cases, the shunt inductance L_s is a sum of the stub inductance and the via inductance. While the original ZOR design uses a via with diameter equal to 0.4 mm, via used in the optimized SSSR is equal to 0.5 mm for fabrication reasons. This results in approximately 10% lower the via inductance, so slightly longer (1%) stub should be used. However, resonators with the unchanged performances could be designed by using vias with a smaller diameter (for example 0.1 mm) and shorter stub lengths. This illustrates well the impact that via dimensions have on the performance of all CRLH-based resonators. To validate the parameter extraction procedure, the responses of electromagnetic simulation and electric model of SRRR are compared in Fig. 3. It can be seen that the electrical model describes EM behaviour very accurately and in a wide frequency range, up to the second harmonic.

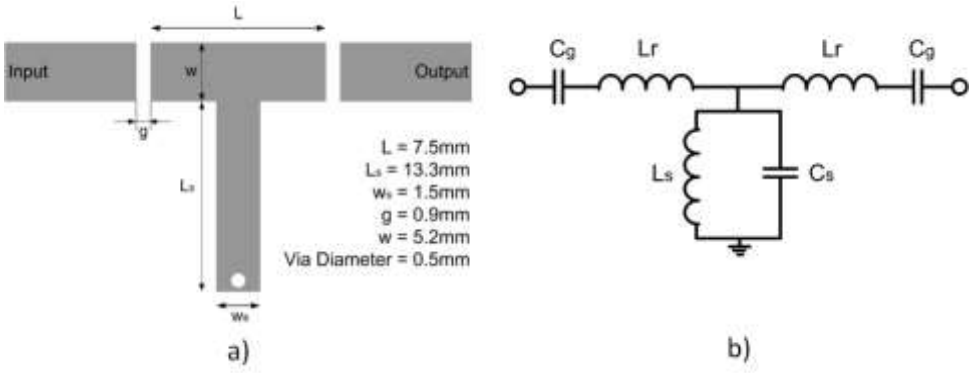

Fig. 1 Single Shunt Stub Resonator (SSSR): (a) Layout with optimized dimensions, (b) Equivalent circuit of the proposed SSSR resonator.

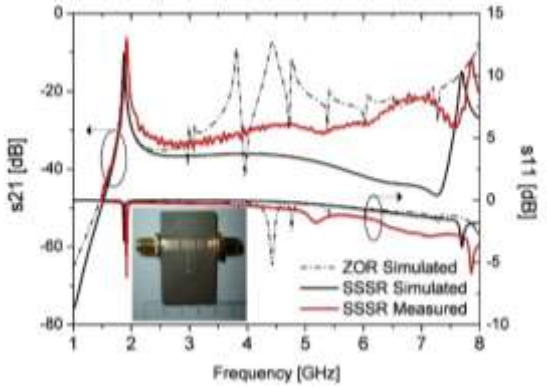

Fig. 2 Comparison of the simulated responses of ZOR and SSSR, and the measured SSSR response. Photograph of fabricated circuit is shown as inset.

Table 1 Extracted equivalent circuit parameters for SSSR and ZOR

	C_q [pF]	L_r [nH]	C_s [pF]	L_s [nH]
SSSR	0.0564	0.874	0.81	8.24
ZOR	0.519	2.58	2	3

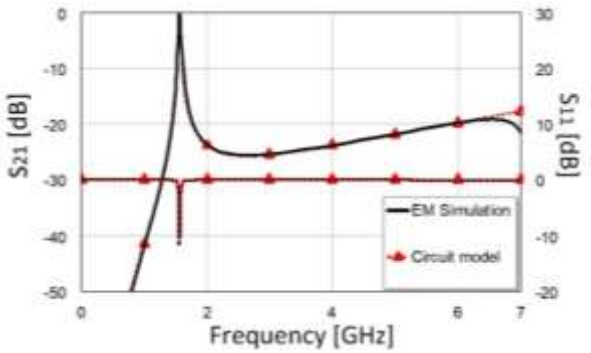

Fig. 3 Comparison of responses obtained from full-wave electromagnetic simulation (EM) and the equivalent circuit model (EL) of SSSR.

3. DUAL-BAND RESONATOR

Due to the small size of the proposed structure, compact dual-band resonators can be designed using superposition of two SSSRs tuned to different frequencies and placed at a distance *s*, Fig. 4a. The equivalent circuit of the proposed dual-band resonator is shown in Fig. 4b. It consists of electric models of two SSSRs, capacitively coupled through C_C. An additional coupling between the feed lines is included in model by C_x. Although very small (C_x<1nF), this additional coupling is responsible for the pole located around 1 GHz in the transmission characteristic of the dual-band resonator. To illustrate applicability of the

proposed dual-band resonator, the dimensions of the resonator have been optimized to obtain center frequency of the passbands equal to 2.4 GHz and 3.5 GHz, i.e. to the frequencies of IEEE WiMAX 802.16 standard. The following dimension of the resonators have been obtained: L=3.5 mm, g=0.1 mm, w_1=1.4 mm, w_2=2.2 mm, w_{s1}=w_{s2}=0.5 mm, L_{s1}=9.6 mm, L_{s2}=14.3 mm, s=1.6 mm, via dimensions equal to 0.15 x 0.15 mm. The simulation response of the proposed dual-band resonator is shown in Fig. 5, together with the measured results. The proposed dual-band resonator is fabricated in standard PCB technology on 1.575 mm thick Taconic substrate with dielectric constant ε_r=2.17. Layout of the fabricated circuit is shown as an inset in Fig. 5. A very good agreement is obtained. The measured insertion losses are equal to -2.68 dB and -2.61 dB, respectively. The 3 dB-fractional bandwidths are somewhat larger than in the simulated case, especially in the second pass band and are equal to 1.91 % and 2.38 %, respectively, and the spurious response is located at approximately four times the resonant frequency. The overall width of the resonator is only 3.5 mm, i.e. λ_g/26, where λ_g is the guided wavelength. The length of the resonator, currently equal to λ_g/3, can be significantly reduced by meandering the inductive stubs.

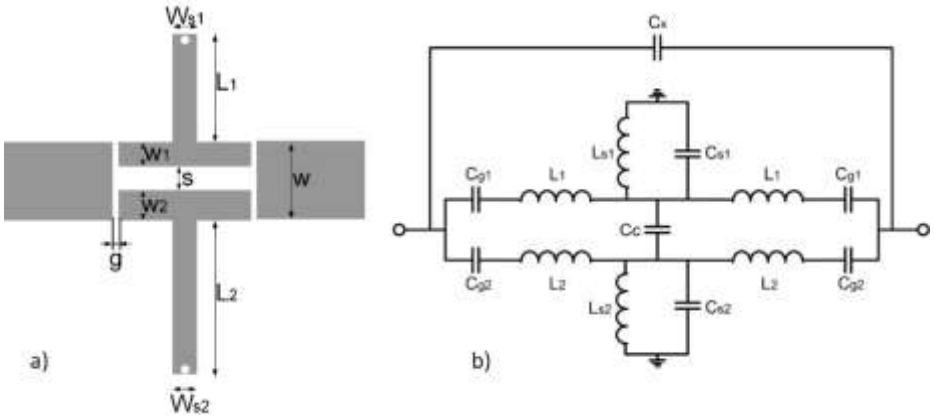

Fig. 4 a) Layout of the proposed dual-band resonator, and b) equivalent circuit model of the proposed dual-band resonator.

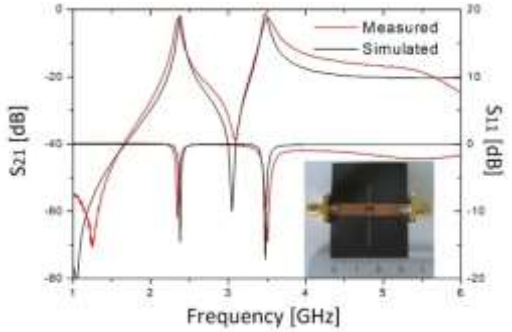

Fig. 5 Measured and simulated responses of the proposed dual-band resonator. Photograph of the fabricated resonator is shown as inset.

4. PARAMETERS ANALYSIS

The response of the proposed dual-band resonator, i.e. its two resonant frequencies, corresponding insertions losses and the bandwidths, can be independently controlled by changing specific geometrical parameters of individual SSSRs. The influence of different geometrical parameters of the dual-band resonator to the performances are analysed in Fig. 6. Simulation results for several different distances between two SSSRs, *s*, are compared in Fig. 6a, while the influence of the stubs length to the resonances is shown in Fig. 6b. It can be seen that the coupling between two SSSRs can be neglected in most cases. Only for very small values of *s*, performance of the dual-band resonator is slightly affected by mutual coupling between two SSSRs. Reducing *s* to the minimal value achievable in the standard PCB technology, equal to 0.1 mm, results in the shifts of resonant frequencies of only 6%.

It is interesting to observe how the total length of the structure *L* influences the performances, Fig. 6b. For example, reducing *L* from 7.5 to 3.5 mm, for fixed all other dimensions, increases the resonant frequency for more than 21%. The limiting situation is also analysed, when the dual-band resonator consists only of two grounded stubs, i.e. $L=w_{s1}=w_{s2}$=0.5mm. The dual-band behaviour is preserved, while the selectivity of the peaks is influenced by increased coupling to the feed lines. Obviously, if two identical SSSRs are used, only one resonant peak arises. Therefore, several mechanisms can be used for tuning the resonant frequencies and the bandwidths. Small changes in the dimensions of the stub L_s and w_s, result in large changes of the resonant frequency and the bandwidths. For example, by reducing stub length from 18 mm to 12 mm, resonant frequency increases for more than 22%, due to decreased stub inductance, Figure 6c. Width of the stub slightly influences on the resonant frequency but dominantly influences on the width of the resonant peak.

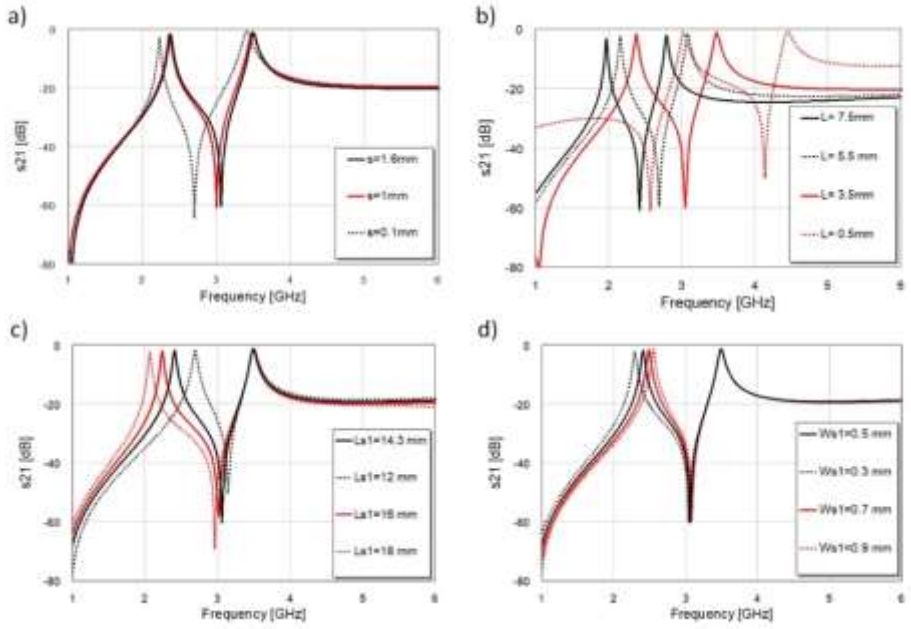

Fig. 6 Influence of the dimensions to the performance of the proposed dual-band resonator: a) the coupling between two SSSRs, b) length of the resonator, *L*, c) length of the stub, L_{S1}, and d) width of the stub, w_{S1}.

Consequently, the resonant frequencies and the bandwidths can be independently set with the proposed optimization of all parameters.

5. DUAL-BAND FILTERS

In order to demonstrate applicability of the proposed dual-band resonators, two dual-band passband filters of the second order have been designed. The layout of the proposed dual-band filter with all relevant dimensions is shown in Figure 7. In order to obtain proper coupling between resonators in each band, i.e. the independent control of the passband characteristics, the feeding lines are slightly modified. One additional segment has been added that allows independent control of the coupling lengths d_1 and d_2.

Filter1 has been designed to operate at 2.4 and 3.5 GHz with the 3 dB fractional bandwidths of 1.2% and 4.7 %, respectively and return losses better than -12 dB in both bands. The geometrical parameter of the filter have been determined as follows: L=3.5 mm, g=0.1 mm, w_1=w_2=2.2 mm, w_{s1}=0.5 mm w_{s2}=0.9 mm, L_{s1}=6.7 mm, L_{s2}=13.5 mm, s=1 mm, d_1=0.75mm, d_2=0.55 mm, and via dimensions are equal to 0.2 mm. The response of the Filter1 is shown in Figure 8a. The simulated insertion losses are -2.5 dB and -1 dB, respectively.

Filter2 has been designed to operate at 3.5 and 5.8 GHz with the 3 dB fractional bandwidths of 3.6 % and 8%, respectively and return losses better than -12 dB in both bands. The optimized geometrical parameters of the filters are: L=3.5 mm, g=0.1 mm, w_1=2.2 mm, w_2=1.9 mm, w_{s1}=0.5 mm w_{s2}=0.1 mm, L_{s1}=6.7 mm, L_{s2}=1.5 mm, s=0.9 mm, d_1=0.8 mm, d_2=0.75 mm, and via dimensions are equal to 0.2 mm. The simulated response of the Filter2 is shown in Figure 8b. The proposed Filter2 shows small insertion losses of -1.3 dB and -1.53 dB, receptively. The size of the Fitler2 is 7.9 mm × 13.2 mm, i.e. 0.13λ_g x 0.21λ_g, where λ_g is the guided wavelength on the given substrate at 3.5 GHz. Both proposed filters exhibit excellent characteristics, high selectivity, and compact dimensions.

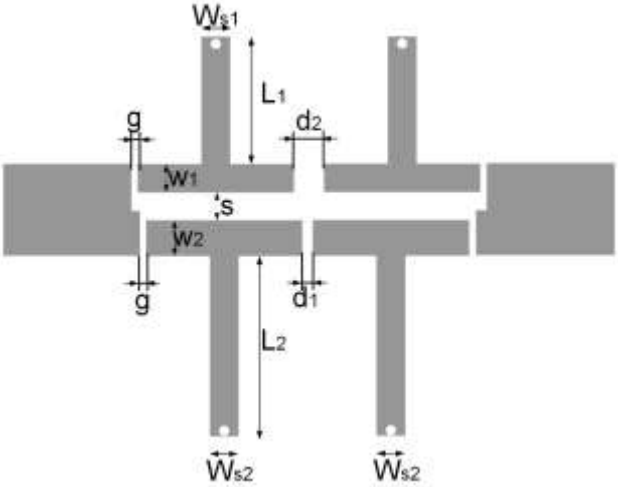

Fig 7 Layout of the second order dual-band passband filter based on SRRRs with all relevant dimensions.

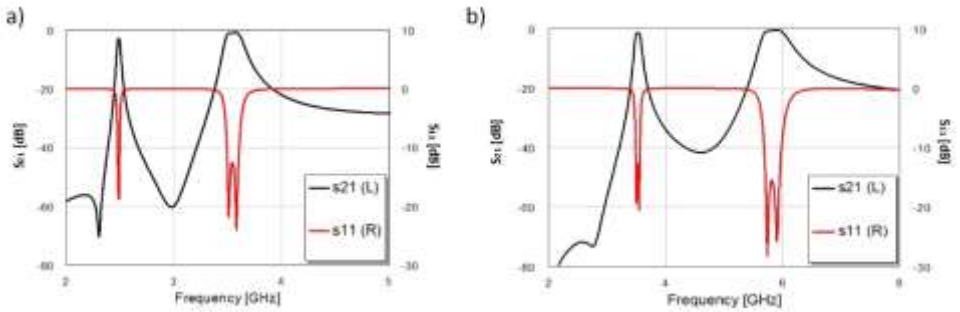

Fig. 8 Response of the second order dual-band passbands filters: a) Filter 1, and b) Filter 2

The proposed filters are compared with recently published microstrip dual-band bandpass filters based on different configurations, [11]-[16]. The characteristic parameters for these filters are summarized in the Table 2, where f_{c1} and f_{c2} denotes central frequencies, and IL_1 and IL_2 are insertion losses, in first and second band, respectively. The size of all filters is shown in guided wavelength, calculated at first resonant frequency. The proposed filters have comparable in-band characteristics and they are more compact than the most of the other filters published so far. Although one may argue that the filter published in [14] has smaller size, it should be noted that these filter has higher insertions losses. The filter published in [15] outperform all other filters in term of insertion losses but its footprint is nearly twice as large as the proposed Filter 2. Additional miniaturization of the proposed filters can be achieved with bending of the inductive stubs. Therefore, the proposed topology presents a good candidate for the design of high-performance dual-band filters since it unifies the requirements for good in-band characteristics and compactness.

Table 2 Comparison of the characteristics of the proposed filters and other recently published dual-band passband filters

Reference Unit	f_{c1} [GHz]	f_{c2} [GHz]	IL_1 [dB]	IL_2 [dB]	Size [λ_g^2]
[11]	2.45	5.25	-2	-2.33	0.245
[12]	2.09	2.62	-1.56	-1.45	0.0377
[13]	2.45	5.8	-2.12	-2.33	0.2346
[14]	2.4	5.2	-1.66	-2.25	0.0143
[15]	2.35	5.68	-0.35	-0.25	0.0452
[16]	2.41	3.52	-2	-2.2	0.0679
Filter 1	2.45	3.5	-2.5	-1	0.052
Filter 2	3.5	5.8	-1.3	-1.53	0.0273

6. CONCLUSION

In this paper, we have proposed novel compact dual-band resonator realized using superposition of two singe shunt stubs. The proposed resonator exhibits spurious response in wide frequency range and therefore allows construction of dual-band filters using the superposition principle. The circuit model and design procedures of a dual-band

resonators have been analysed in details and verified through two fabricated prototypes. As an examples, two dual-band bandpass filters that operate simultaneously at the WiMAX frequency bands are designed. Designed Filter1 is characterized with center operating frequencies of 2.4 GHz and 3.5 GHz, with return losses better than 12 dB in both bands, and the 3 dB fractional bandwidths equal to 1.2% and 4.7%, respectively. Filter2 is characterized with central frequencies of equal to 3.5 GHz and 5.8 GHz with fractional bandwidths of 3.6% and 8%, receptively, and return losses better than 12 dB in both bands. The proposed filters exhibit excellent in-band characteristics, spurious response, high selectivity, and compact dimensions.

Acknowledgement: *This work has been supported by Ministry of Education, Science and Technological Development, Republic of Serbia within the project III 44006 - Development of new information and communication technologies, based on advanced mathematical methods, with applications in medicine, telecommunications, power systems, protection of national heritage and education.*

REFERENCES

[1] P. Ma, B. Wei, J. Hong, Z. Xu, X. Guo, B. Cao, and L. Jiang, "A Design Method of Multimode Multiband Bandpass Filters," *IEEE Trans. Microw Theory Tech.*, vol. 66, no. 6, pp. 2791–2799, Mar. 2018.

[2] J.-X. Chen, J. Li and J. Shi, "Miniaturized Dual-Band Differential Filter Using Dual-Mode Dielectric Resonator," *IEEE Microw. Wirel. Comp. Lett.*, vol. 28, no. 8, pp. 657–659, Aug. 2018.

[3] H. Liu, Y. Song, B. Ren, P. Wen, X. Guan, H. Xu, "Balanced Tri-Band Bandpass Filter Design Using Octo-Section Stepped-Impedance Ring Resonator With Open Stubs," *IEEE Microw. Wirel. Comp. Lett.*, vol. 27, no. 10, pp. 912–914, Oct. 2017.

[4] F. Capolino, *Applications of Metamaterials.* Boca Raton: CRC Press, Taylor & Francis group, 2009.

[5] A. Lai, T. Itoh and C. Caloz, "Composite right/left-handed transmission line metamaterials," IEEE Microw. Magazine, vol. 5, no. 3, pp. 34–50, Sept. 2004.

[6] C. Caloz, H. Okabe, T. Iwai, and T. Itoh, "Transmission line approach of left-handed (LH) materials," in *Proc. USNC/URSI National Radio Science Meeting*, San Antonio, TX, June 2002, vol. 1, p. 39.

[7] G.V. Eleftheriades, O. Siddiqui, and A.K. Iyer, "Transmission line models for negative refractive index media and associated implementations without excess resonators," *IEEE Microwave Wireless Compon. Lett.*, vol. 13, pp. 51–53, Feb. 2003

[8] Caloz and T. Itoh, "Electromagnetic Metamaterials: Transmission Line Theory and Microwave Applications," *John Wiley & Sons, Inc*, 2006.

[9] A. Sanada, C. Caloz, and T. Itoh, "Zeroth order resonance in composite right/left-handed transmission line resonators," In Proc. of the Asia-Pacific Microwave Conf., Seoul, Korea, 2003, vol. 3, pp. 1588–1592.

[10] G. Sisó, M. Gil, J. Bonache and F. Martín, "Generalized Model for Multiband Metamaterial Transmission Lines," *IEEE Microwave and Wireless Components letters*, vol. 18, no. 11, pp. 728–730, November 2008.

[11] C.-H. Lee, C.-I. G. Hsu, and C.-C. Hsu, "Balanced Dual-Band BPF With Stub-Loaded SIRs for Common-Mode Suppression," *IEEE Microwave and Wireless Components letters*, vol. 20, no. 2, pp. 70–72, February, 2010.

[12] X.B. Wei, G.T. Yue, J.X Liao, P. Wang, Z. Q. Xu, Y. Shi, "Compact dual-band bandpass filter with ultra-wide upper-stopband," *Electron Letters*, vol. 49, pp. 708–709, 2013.

[13] M. Jiang, L.M. Chang, A. Chin, "Design of dual-passband microstrip bandpass filters with multi-spurious suppression," *IEEE Microwave and Wireless Components letters*, vol. 20, pp. 199–201, 2010.

[14] J. Luo, C. Liao, H. Zhou, X. Xiong, "A novel miniature dual-band bandpass filter based on the first and second resonances for 2.4/ 5.2 GHz WLAN application," *Microwave and Optical Technology Letters*, vol. 57, pp. 1143–1146, 2015.

[15] M. R. Salehi, E. Abiri, L. Noori, "Design of a microstrip dual-band bandpass filter with compact size and tunable resonance frequencies for WLAN applications," *International Journal of Computer and Electrical Engineering*, vol. 6, pp. 248–251, 2014

[16] K. Song, F. Zhang, Y. Fan, "Miniaturized dual-band bandpass filter with good frequency selectivity using SIR and DGS," *International Journal of Electronics and Communications*, vol. 68, pp. 384–387, 2014.